Statistical treatment of detection cross-section uncertainties in the analysis of solar neutrino data

M.V. Garzelli and C. Giunti

INFN, Sez. di Torino, and Dip. di Fisica Teorica, Univ. di Torino, I–10125 Torino, Italy (June 13, 2000)

Abstract

We propose a modification to the standard statistical treatment of the detection cross-section uncertainties in the analysis of solar neutrino data. We argue that the uncertainties of the energy-averaged cross sections of the different neutrino fluxes in the same experiment should be treated as correlated. We show that the resulting allowed regions for the neutrino oscillation parameters are significantly larger than the ones obtained with uncorrelated uncertainties.

PACS numbers: 26.65.+t, 14.60.Pq, 14.60.Lm

Typeset using REVT_{EX}

The discrepancy between solar neutrino data [1-4] and the predictions of the Standard Solar Model (SSM) [5], known as the "solar neutrino problem", represents one of the evidences in favor of neutrino oscillations (see [6]). The statistical analysis of solar neutrino data allow to obtain information on the values of the neutrino oscillation parameters. The latest solar neutrino data [1-4] have been analyzed in the framework of two-neutrino mixing [7-9], three-neutrino mixing [9] and four-neutrino mixing [10].

One of the crucial ingredients in the analysis of solar neutrino data is the calculation of the statistical covariance matrix V of the uncertainties. This matrix determines the χ^2 of the fit through the formula

$$\chi^2 = \sum_{j_1, j_2} \left(R_{j_1}^{(\text{thr})} - R_{j_1}^{(\text{exp})} \right) (V^{-1})_{j_1 j_2} \left(R_{j_2}^{(\text{thr})} - R_{j_2}^{(\text{exp})} \right) \,. \tag{1}$$

Here $R_j^{(\text{exp})}$ is the event rate measured in the j^{th} experiment and $R_j^{(\text{thr})}$ is the corresponding theoretical event rate, that depends on the neutrino fluxes predicted by the SSM and on the properties of neutrinos that modify the flux along the neutrino propagation. In the case of two-neutrino oscillations the theoretical event rate depends on the mass-squared difference $\Delta m^2 \equiv m_2^2 - m_1^2$ and on the mixing angle ϑ (see [6]).

The covariance matrix V includes the uncertainties of the experimental rates $R_j^{(exp)}$, and the uncertainties of the theoretical rates $R_j^{(thr)}$, quantified by the experimental and theoretical covariance matrices $V^{(exp)}$ and $V^{(thr)}$, respectively. Since experimental and theoretical errors are independent, the corresponding uncertainties can be added in quadrature:

$$V = V^{(\exp)} + V^{(\operatorname{thr})} \,. \tag{2}$$

Here we are concerned with the covariance matrix of theoretical uncertainties, $V^{(\text{thr})}$, that can be written as the sum of two independent contributions,

$$V^{(\rm thr)} = V^{(\rm cs)} + V^{(\rm fx)}, \qquad (3)$$

where $V^{(cs)}$ is the covariance matrix of the errors due to the uncertainties of the detection cross sections and $V^{(fx)}$ is the covariance matrix of the errors due to the uncertainties of the neutrino fluxes. Very convenient expressions for these matrices have been presented in Refs. [11,9]. These expressions have been used by many authors for the statistical analysis of solar neutrino data in terms of neutrino oscillations [9,12,8,7,10,13–15].

Here we would like to examine closely the expression given in [11,9] for the covariance matrix of the detection cross section:

$$V_{j_1 j_2}^{(cs)} = \delta_{j_1 j_2} \sum_{i} \left(R_{i j_1}^{(thr)} \Delta \ln C_{i j_1} \right)^2 , \qquad (4)$$

where R_{ij} is the event rate in the detector j due to the neutrino flux produced in the i^{th} thermonuclear reaction in the sun (i = pp, pep, Hep, Be, B, N, O, F) and C_{ij} is the corresponding energy-averaged cross section. The quantity $\Delta \ln C_{ij} = \Delta C_{ij}/C_{ij}$ is the relative uncertainty of the cross section C_{ij} , whose value is given in Ref. [9].

The expression (4) is based on two assumptions: 1) the errors of the detection cross sections in different experiment are independent; 2) the errors of energy-averaged cross

section of the different neutrino fluxes in the same experiment are uncorrelated. Indeed, in Eq. (4) the errors of energy-averaged cross section of the different neutrino fluxes in the same experiment, $R_{ij}^{(\text{thr})}\Delta \ln C_{ij}$, are added in quadrature to the corresponding diagonal element $V_{jj}^{(\text{cs})}$.

We think that the first assumption is appropriate, but the second one is questionable. This is due to the fact that the correlations between the uncertainties of each detection cross section at different energies is not known. Moreover, the uncertainties of the energy-averaged cross section of the neutrino fluxes that have an overlap of energy ranges are certainly not uncorrelated.

Since the correlations of the errors of energy-averaged cross section of the different neutrino fluxes in the same experiment are not known, the correct attitude consists in adopting the most conservative approach, assuming a complete correlation. In this case the errors must be added linearly:

$$V_{j_1 j_2}^{(cs)} = \delta_{j_1 j_2} \left(\sum_{i} R_{i j_1}^{(thr)} \Delta \ln C_{i j_1} \right)^2 \,. \tag{5}$$

This approach has been also recommended in Ref. [16], that is the standard reference for the detection cross section in Gallium experiments. Let us notice that it reflects a rather realistic possibility: that in which the errors of the cross section in a given experiment have the same sign at all energies.

We have performed a fit of the total rates measured in solar neutrino experiments in terms of oscillations between two active neutrinos ($\nu_e \rightarrow \nu_{\mu}$ or $\nu_e \rightarrow \nu_{\tau}$) in order to study the change of the allowed regions for the neutrino oscillation parameters Δm^2 and ϑ when the expression (5) for $V^{(cs)}$ is used in place of Eq. (4). The results of our fits are presented in Figs. 1–5. We have used the latest measurements of the event rates in the Homestake [1] and Super-Kamiokande [4] experiments, and the weighted average of the rates measured in the two Gallium experiments GALLEX [2] and SAGE [3]. The values of these rates are given in Table I of Ref. [7].

Our calculation of the theoretical event rates $R_{ij}^{(\text{thr})}$ follows the standard method described in several papers for matter-enhanced MSW transitions [17–19] and vacuum oscillations [20,19]. We calculate the MSW survival probability of ν_e 's in the Sun using the standard analytic prescription [21,18,17,6] and the level-crossing probability appropriate for an exponential density profile [22,17]. We calculate the regeneration in the Earth using a two-step model of the Earth density profile, that is known to produce results that do not differ appreciably from those obtained with the correct density profile. We have used the tables of neutrino fluxes, solar density and radiochemical detector cross sections available in Bahcall's web page [23]. We have neglected the matter effects that slightly affect the vacuum oscillation solutions of the solar neutrino problem, as discussed in [14,12]. In Figs. 1–5 we have used as abscissa the parameter $\tan^2 \vartheta$ that allows a better view of the regions at large mixing angles with respect to the usual parameter $\sin^2 2\vartheta$. The parameter $\tan^2 \vartheta$ has been employed in the past in the framework of three-neutrino mixing [24–26] and its use in the framework of two-neutrino mixing has been recently advocated in [15] because it allows to explore the possible presence of allowed regions with $\vartheta > \pi/4$. The allowed regions in Figs. 1–5 are calculated through the constraint $\chi^2 \leq \chi^2_{\min} + \Delta \chi^2(\alpha)$, where χ^2_{\min} is the global minimum of the χ^2 , $\chi^2_{\min} = 0.42$ for $\Delta m^2 = 5.1 \times 10^{-6} \,\mathrm{eV}^2$ and $\tan^2 \vartheta = 1.6 \times 10^{-3}$ in both cases of uncorrelated (Eq. (4)) and correlated (Eq. (5)) cross section uncertainties. We consider confidence levels $\alpha = 0.90, 0.95, 0.99$ (the regions inside the solid, short-dashed and long-dashed contours, respectively) for two degrees of freedom, which give $\Delta \chi^2(0.90) = 4.61, \Delta \chi^2(0.95) = 5.99$, and $\Delta \chi^2(0.99) = 9.21$.

The linear addition in (5) of the uncertainties of the detection cross section lead to larger values of the diagonal elements of the covariance matrix V and to smaller values of the χ^2 in Eq. (1), with respect to the case of uncorrelated uncertainties (Eq. (4)). Since the variation of χ^2 in the space of the neutrino oscillation parameters $\tan^2 \vartheta$, Δm^2 near the minimum of the χ^2 is proportional to V^{-1} (the contribution of the variation of V^{-1} is negligible near the minimum),

$$\delta\chi^2 \simeq 2\sum_{j_1,j_2} \left(R_{j_1}^{(\text{thr})} - R_{j_1}^{(\text{exp})} \right) (V^{-1})_{j_1j_2} \left(\frac{\partial R_{j_2}^{(\text{thr})}}{\partial (\tan^2 \vartheta)} \,\delta(\tan^2 \vartheta) + \frac{\partial R_{j_2}^{(\text{thr})}}{\partial (\Delta m^2)} \,\delta(\Delta m^2) \right) \,, \quad (6)$$

the slope of the χ^2 is smaller in the case of correlated uncertainties (Eq. (5)) than in the case of uncorrelated uncertainties (Eq. (4)). Therefore, we expect to obtain larger allowed regions in the case of correlated uncertainties, with respect to those obtained with uncorrelated uncertainties.

Figures 1 and 2 show the MSW allowed regions obtained using the expressions (4) and (5) for $V^{(cs)}$, respectively. One can see that all the three MSW allowed regions, usually called SMA (for $\Delta m^2 \simeq 5 \times 10^{-6} \,\mathrm{eV}^2$ and $\tan^2 \vartheta \simeq 10^{-3}$), LMA (for $\Delta m^2 \simeq 2 \times 10^{-5} \,\mathrm{eV}^2$ and $\tan^2 \vartheta \simeq 0.3$) and LOW (for $\Delta m^2 \simeq 10^{-7} \,\mathrm{eV}^2$ and $\tan^2 \vartheta \simeq 0.5$), are larger when the expressions (5) with correlated cross section uncertainties is used. The minimum and maximum values of $\tan^2 \vartheta$ and Δm^2 in the 99% CL allowed regions in Fig. 1 (unc) and Fig. 2 (cor) are listed in Table I and the difference between these regions is illustrated in Fig. 3. One can see that the SMA-cor region is slightly larger than the SMA-unc region. The LMA-cor region is appreciably larger than the LMA-unc region, allowing values of Δm^2 and $\tan^2 \vartheta$ as high as $3.5 \times 10^{-4} \,\mathrm{eV}^2$ and 0.82, in contrast to the upper limits $2.4 \times 10^{-4} \,\mathrm{eV}^2$ and 0.67 for the LMA-unc region. The larger effects occur in the LOW region. In the LOW-cor region $\tan^2 \vartheta$ can be as large as 1, corresponding to maximal mixing, and $2.4 \times 10^{-8} \,\mathrm{eV}^2 \leq \Delta m^2 \leq 3.5 \times 10^{-7} \,\mathrm{eV}^2$.

Figures 4 and 5 show the vacuum oscillation allowed regions obtained with uncorrelated (Eq. (4)) and correlated (Eq. (5)) cross section uncertainties, respectively. One can see that the allowed regions obtained with correlated cross section uncertainties are significantly larger that the ones obtained with uncorrelated cross section uncertainties. For example, the 99% CL allowed region at $\Delta m^2 \simeq 5 \times 10^{-10} \,\mathrm{eV}^2$ is considerably larger with correlated cross section uncertainties (Fig. 5) than with uncorrelated ones (Fig. 4), and the 90% CL allowed region in Fig. 5 at $\Delta m^2 \simeq 2.7 \times 10^{-10} \,\mathrm{eV}^2$ does not exist in Fig. 4.

In conclusion, we have proposed a modification of the standard statistical treatment of the detection cross-section uncertainties in the analysis of solar neutrino data. We have argued that, because of lack of information, a conservative approach should be used in the treatment of the correlations between the energy-averaged cross sections of the different neutrino fluxes in the same experiment, leading to the assumption of correlated errors and to a linear addition of the uncertainties. We have shown in Figs. 1–5 that the resulting allowed regions for the neutrino oscillation parameters are significantly larger than those obtained with uncorrelated detection cross sections uncertainties. We think that the appropriate treatment of the detection cross section uncertainties proposed here will be rather important in the future, when more precise solar neutrino data obtained in the Super-Kamiokande, SNO [27], Borexino [28], GNO [29] and other experiments will be published.

ACKNOWLEDGMENTS

We would like to thank A. Bottino for useful suggestions and encouragement. C.G. would like to thank P. Krastev, E. Lisi, H. Murayama and S. Petcov for useful discussions on the fit of solar neutrino data.

REFERENCES

- [1] B. T. Cleveland *et al.*, Astrophys. J. **496**, 505 (1998).
- [2] GALLEX, W. Hampel *et al.*, Phys. Lett. **B447**, 127 (1999).
- [3] SAGE, J. N. Abdurashitov *et al.*, Phys. Rev. C60, 055801 (1999), arXiv:astroph/9907113.
- [4] Y. Suzuki (Super-Kamiokande Coll.), Talk presented at the XIX Int. Symposium on Lepton and Photon Interactions at High Energies, Stanford, Aug. 1999 (http://lp99.slac.stanford.edu).
- [5] J. N. Bahcall, S. Basu, and M. H. Pinsonneault, Phys. Lett. B433, 1 (1998), arXiv:astroph/9805135.
- [6] S. M. Bilenky, C. Giunti, and W. Grimus, Prog. Part. Nucl. Phys. 43, 1 (1999), arXiv:hep-ph/9812360.
- [7] M.C. Gonzalez-Garcia, P.C. de Holanda, C. Pena-Garay and J.W.F. Valle, arXiv:hepph/9906469.
- [8] J.N. Bahcall, P.I. Krastev and A.Yu. Smirnov, arXiv:hep-ph/9911248.
- [9] G. L. Fogli, E. Lisi, D. Montanino, and A. Palazzo, Phys. Rev. D62, 013002 (2000), arXiv:hep-ph/9912231.
- [10] C. Giunti, M.C. Gonzalez-Garcia and C. Pena-Garay, arXiv:hep-ph/0001101.
- [11] G. L. Fogli and E. Lisi, Astropart. Phys. 3, 185 (1995).
- [12] G.L. Fogli, E. Lisi, D. Montanino and A. Palazzo, arXiv:hep-ph/0005261.
- [13] M.C. Gonzalez-Garcia and C. Pena-Garay, arXiv:hep-ph/0002186.
- [14] A. Friedland, arXiv:hep-ph/0002063.
- [15] A. de Gouvea, A. Friedland and H. Murayama, arXiv:hep-ph/0002064.
- [16] J. N. Bahcall, Phys. Rev. C56, 3391 (1997), arXiv:hep-ph/9710491.
- [17] T. K. Kuo and J. Pantaleone, Rev. Mod. Phys. **61**, 937 (1989).
- [18] P. I. Krastev and S. T. Petcov, Phys. Lett. **B207**, 64 (1988).
- [19] P. I. Krastev and S. T. Petcov, Phys. Lett. **B299**, 99 (1993).
- [20] P. I. Krastev and S. T. Petcov, Phys. Lett. **B285**, 85 (1992).
- [21] S. J. Parke, Phys. Rev. Lett. 57, 1275 (1986).
- [22] S. T. Petcov, Phys. Lett. **B200**, 373 (1988).
- [23] J.N. Bahcall, WWW page: http://www.sns.ias.edu/~jnb/.
- [24] G. L. Fogli, E. Lisi, and G. Scioscia, Phys. Rev. **D52**, 5334 (1995), hep-ph/9506350.
- [25] G. L. Fogli, E. Lisi, and D. Montanino, Phys. Rev. D54, 2048 (1996), arXiv:hepph/9605273.
- [26] G. L. Fogli, E. Lisi, D. Montanino, and G. Scioscia, Phys. Rev. D56, 4365 (1997), hep-ph/9706230.
- [27] J. Boger *et al.*, arXiv:nucl-ex/9910016.
- [28] Borexino, F. von Feilitzsch, Prog. Part. Nucl. Phys. 40, 123 (1998).
- [29] GALLEX and GNO, T. A. Kirsten, Nucl. Phys. Proc. Suppl. 77, 26 (1999).

TAI	BLES
-----	------

	$\tan^2 \vartheta_{\min}$	$\tan^2 \vartheta_{\max}$	$\Delta m_{\min}^2 \; (\mathrm{eV}^2)$	$\Delta m_{\rm max}^2 ~({\rm eV}^2)$
$\operatorname{SMA-unc}$	3.3×10^{-4}	2.9×10^{-3}	3.8×10^{-6}	1.0×10^{-5}
SMA-cor	$3.0 imes 10^{-4}$	3.2×10^{-3}	$3.8 imes 10^{-6}$	1.0×10^{-5}
LMA-unc	0.14	0.67	6.2×10^{-6}	2.4×10^{-4}
LMA-cor	0.14	0.82	$5.6 imes 10^{-6}$	$3.5 imes 10^{-4}$
LOW-unc	0.45	0.82	5.6×10^{-8}	2.6×10^{-7}
LOW-cor	0.41	1.0	2.4×10^{-8}	3.5×10^{-7}

TABLE I. Minimum and maximum values of $\tan^2 \vartheta$ and Δm^2 in the 99% CL allowed regions in Fig. 1 (unc rows) and in Fig. 2 (cor rows).

FIGURES

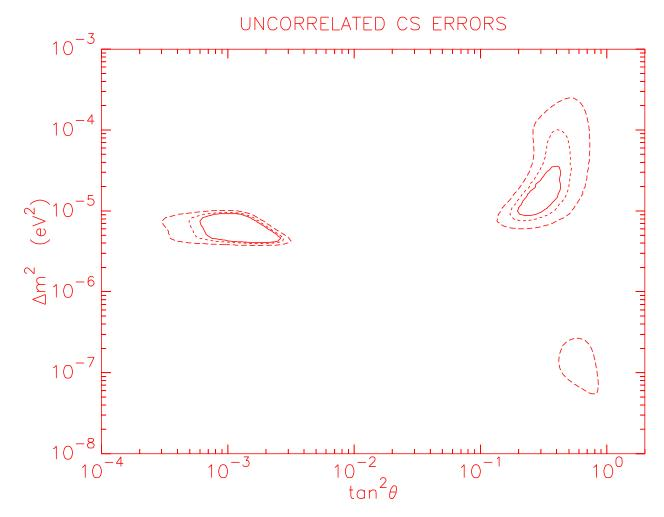


FIG. 1. Allowed regions for the neutrino oscillation parameters Δm^2 and $\tan^2 \vartheta$ in the case of MSW resonant transitions in the Sun and uncorrelated detection cross section uncertainties (Eq. (4)). The regions inside the solid, short-dashed and long-dashed contours are allowed, respectively, at 90%, 95% and 99% confidence level.

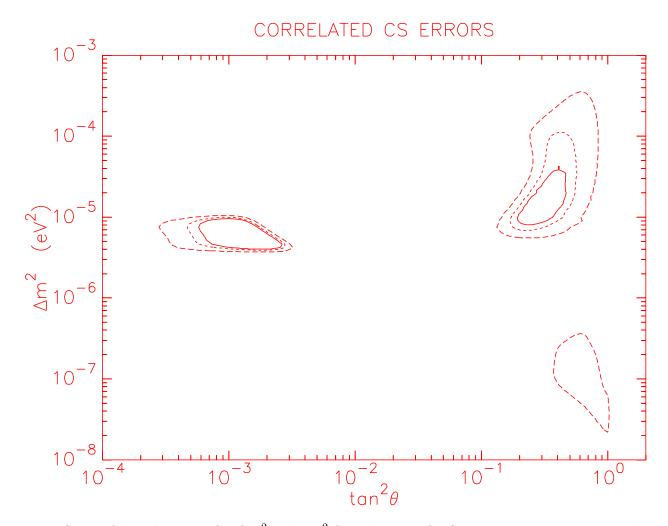


FIG. 2. Allowed regions for Δm^2 and $\tan^2 \vartheta$ in the case of MSW resonant transitions in the Sun and correlated detection cross section uncertainties (Eq. (5)). The regions inside the solid, short-dashed and long-dashed contours are allowed, respectively, at 90%, 95% and 99% confidence level.

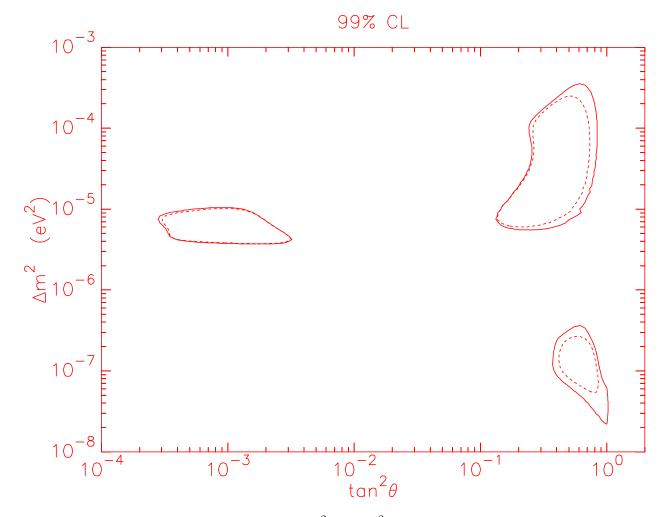


FIG. 3. Allowed regions at 99% CL for Δm^2 and $\tan^2 \vartheta$ in the case of MSW resonant transitions in the Sun. The regions within the solid and dashed contours have been obtained, respectively, with correlated (Eq. (5)) and uncorrelated (Eq. (4)) detection cross section uncertainties.



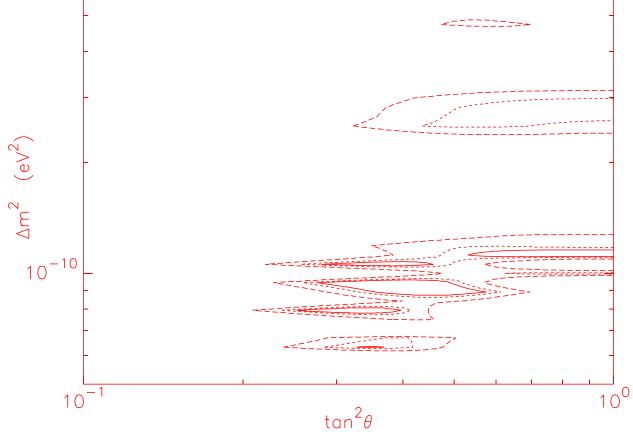


FIG. 4. Allowed regions for the neutrino oscillation parameters Δm^2 and $\tan^2 \vartheta$ in the case of vacuum oscillations from the Sun to the Earth and uncorrelated detection cross section uncertainties (Eq. (4)). The regions inside the solid, short-dashed and long-dashed contours are allowed, respectively, at 90%, 95% and 99% confidence level.

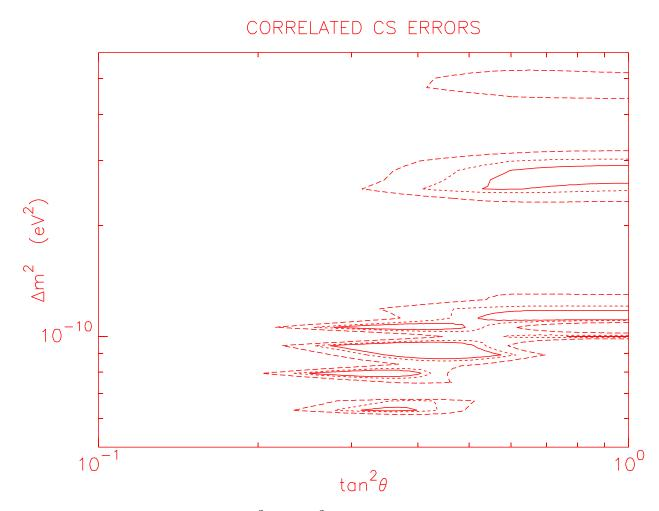


FIG. 5. Allowed regions for Δm^2 and $\tan^2 \vartheta$ in the case of vacuum oscillations from the Sun to the Earth and correlated detection cross section uncertainties (Eq. (5)). The regions inside the solid, short-dashed and long-dashed contours are allowed, respectively, at 90%, 95% and 99% confidence level.